NMM Dynamic Core and HWRF

Zavisa Janjic and Matt Pyle
NOAA/NWS/NCEP/EMC, NCWCP, College Park, MD

Basic Principles

- Forecast accuracy
- Fully compressible equations
- Discretization methods that minimize generation of computational noise and reduce or eliminate need for numerical filters
- Computational efficiency, robustness

Nonhydrostatic *Mesoscale* Model (NMM)

- Built on NWP and regional climate experience by relaxing hydrostatic approximation (Janjic et al., 2001, MWR; Janjic, 2003, MAP, Janjic et al., 2010)
- Add-on nonhydrostatic module
  - Easy comparison of hydrostatic and nonhydrostatic solutions
  - Reduced computational effort at lower resolutions
- General terrain following vertical coordinate based on pressure (non-divergent flow remains on constant pressure surfaces)

Inviscid Adiabatic Equations

π Hydrostatic pressure

p Nonhydrostatic pressure

$\mu = \pi_{Sfc} - \pi_T$ Difference between hydrostatic pressures at surface and top

$$\pi(x,y,s,t) = \pi_T + \sigma_1(s)\Pi + \sigma_2(s)\mu(x,y,t)$$

Π Constant depth of hydrostatic pressure layer at the top

σ_1 Zero at top and bottom of model atmosphere

σ_2 Increases from 0 to 1 from top to bottom

$\alpha = RT/p$ Gas law

$\frac{\partial \Phi}{\partial \pi} = -\alpha$ Hypsometric (not "hydrostatic") Eq.

$$\left[\frac{\partial}{\partial t}\left(\frac{\partial \pi}{\partial s}\right)\right]_s + \nabla_s \cdot \left(\mathbf{v}\frac{\partial \pi}{\partial s}\right) + \frac{\partial}{\partial s}\left(\dot{s}\frac{\partial \pi}{\partial s}\right) = 0$$ Hydrostatic continuity Eq.

Continued ...

Inviscid Adiabatic Equations, contd.

$$w \equiv \frac{dz}{dt} = \frac{1}{g}\left[\left(\frac{\partial \Phi}{\partial t}\right)_s + \mathbf{v}\cdot\nabla_s \Phi + \left(\dot{s}\frac{\partial \pi}{\partial s}\right)\frac{\partial \Phi}{\partial \pi}\right] + W(x,y,t)$$

Integral of nonhydrostatic continuity Eq.

$$\varepsilon \equiv \frac{1}{g}\frac{dw}{dt} = \frac{1}{g}\left[\left(\frac{\partial w}{\partial t}\right)_s + \mathbf{v}\cdot\nabla_s w + \left(\dot{s}\frac{\partial \pi}{\partial s}\right)\frac{\partial w}{\partial \pi}\right]$$

Vertical acceleration

$$\frac{\partial p}{\partial \pi} = 1 + \varepsilon$$

Third Eq. of motion

$$\frac{d\mathbf{v}}{dt} = -(1+\varepsilon)\nabla_s \Phi - \alpha \nabla_s p + f\mathbf{k}\times\mathbf{v}$$

Momentum Eq.

$$\frac{\partial T}{\partial t} = -\mathbf{v}\cdot\nabla_s T - \left(\dot{s}\frac{\partial \pi}{\partial s}\right)\frac{\partial T}{\partial \pi} + \frac{\alpha}{c_p}\left[\frac{\partial p}{\partial t} + \mathbf{v}\cdot\nabla_s p + \left(\dot{s}\frac{\partial \pi}{\partial s}\right)\frac{\partial p}{\partial \pi}\right]$$

Thermodynamic Eq.

Nonhydrostatic Dynamics Specifics

- Φ, w, ε are not independent, no independent prognostic equation for w!
- More complex numerical algorithm, but no over-specification of w
- ε <<1 in meso and large scale atmospheric flows
- Impact of nonhydrostatic dynamics becomes detectable at resolutions <10km, important at 1km.

Horizontal Coordinate System, Rotated Lat-Lon

- Rotates the Earth's latitude and longitude so that the intersection of the Equator and the prime meridian is in the center of the domain
  - Minimized convergence of meridians
  - More uniform grid spacing than on a regular lat-lon grid
  - Allows longer time step than on a regular lat-lon grid

Sample rotated lat-lon domain

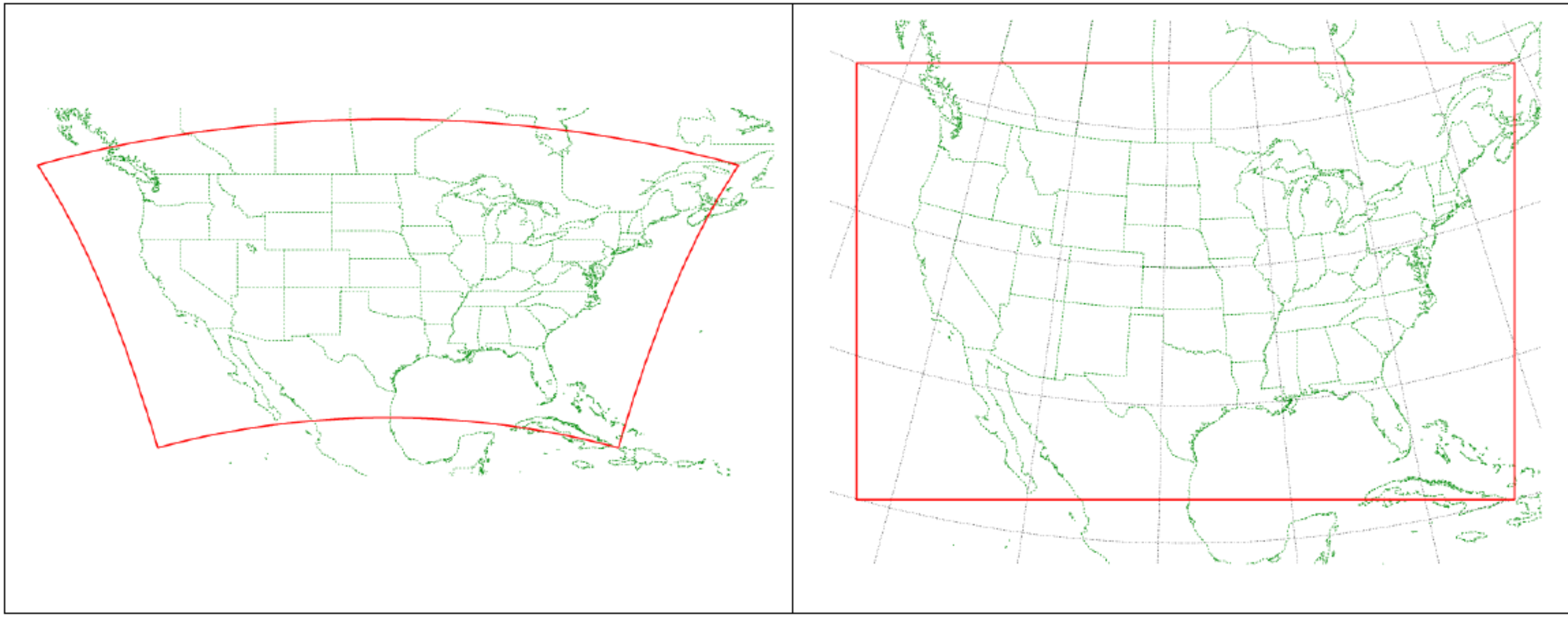

On a regular lat-lon map background

On a rotated lat-lon map background (same rotation as model grid).

Horizontal E grid

h	**v**	h	**v**	h
v	h	**v**	h	**v**
h	**v**	h	**v**	h
v	h	**v**	h	**v**
h	**v**	h	**v**	h

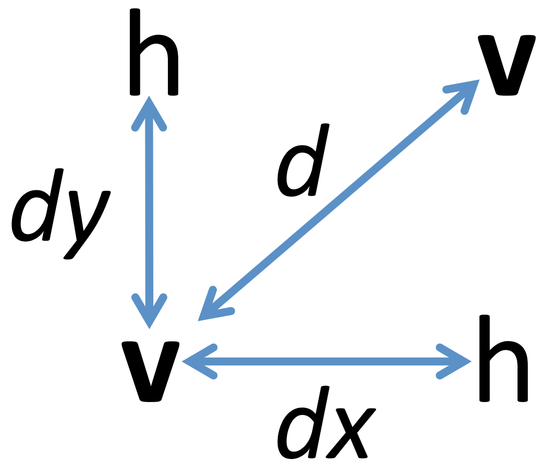

Vertical Coordinate

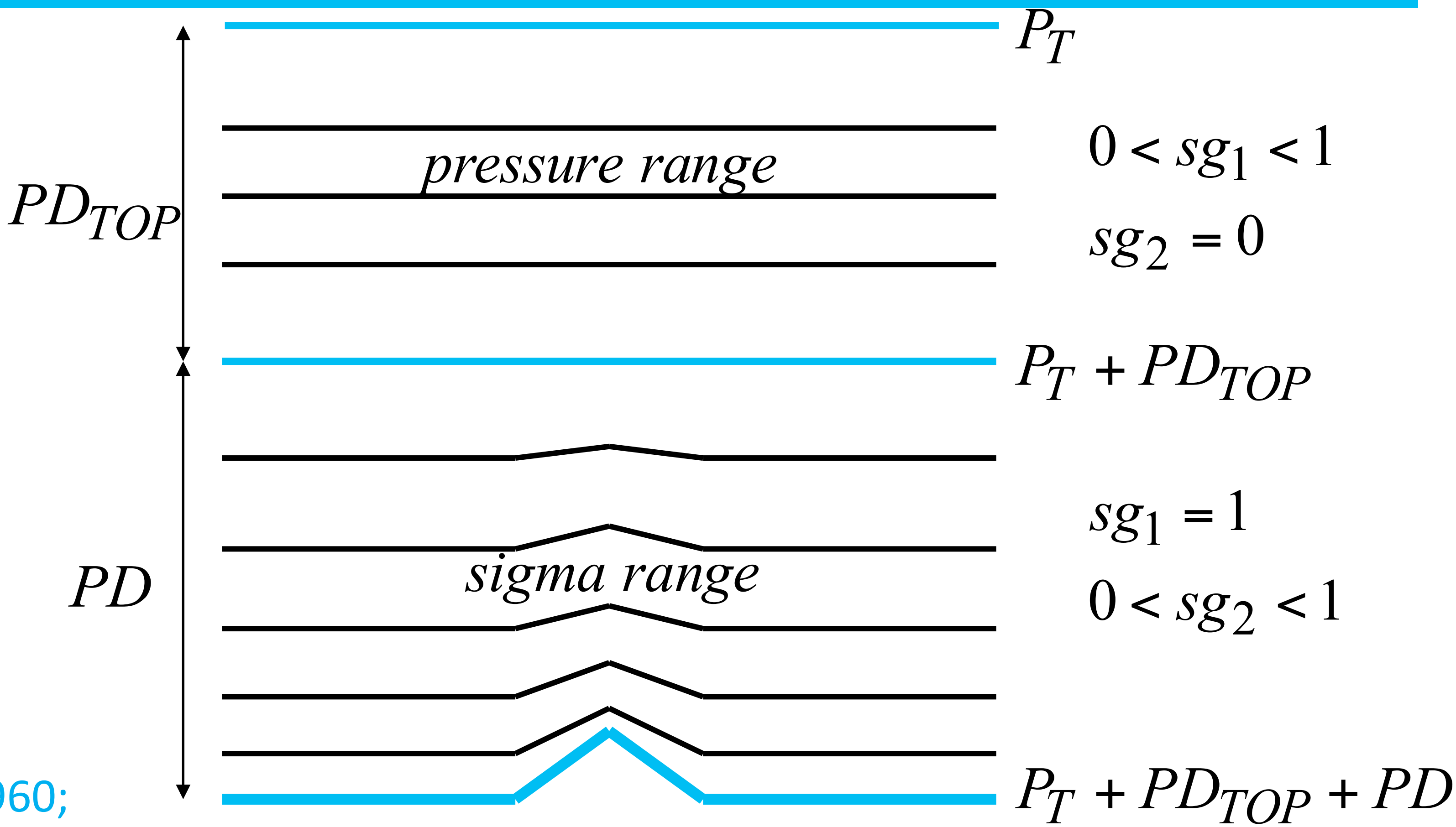

Sangster, 1960;
Arakawa &
Lamb, 1977

$$p = P_T + sg_1\, PD_{TOP} + sg_2\, PD$$

Vertical Staggering

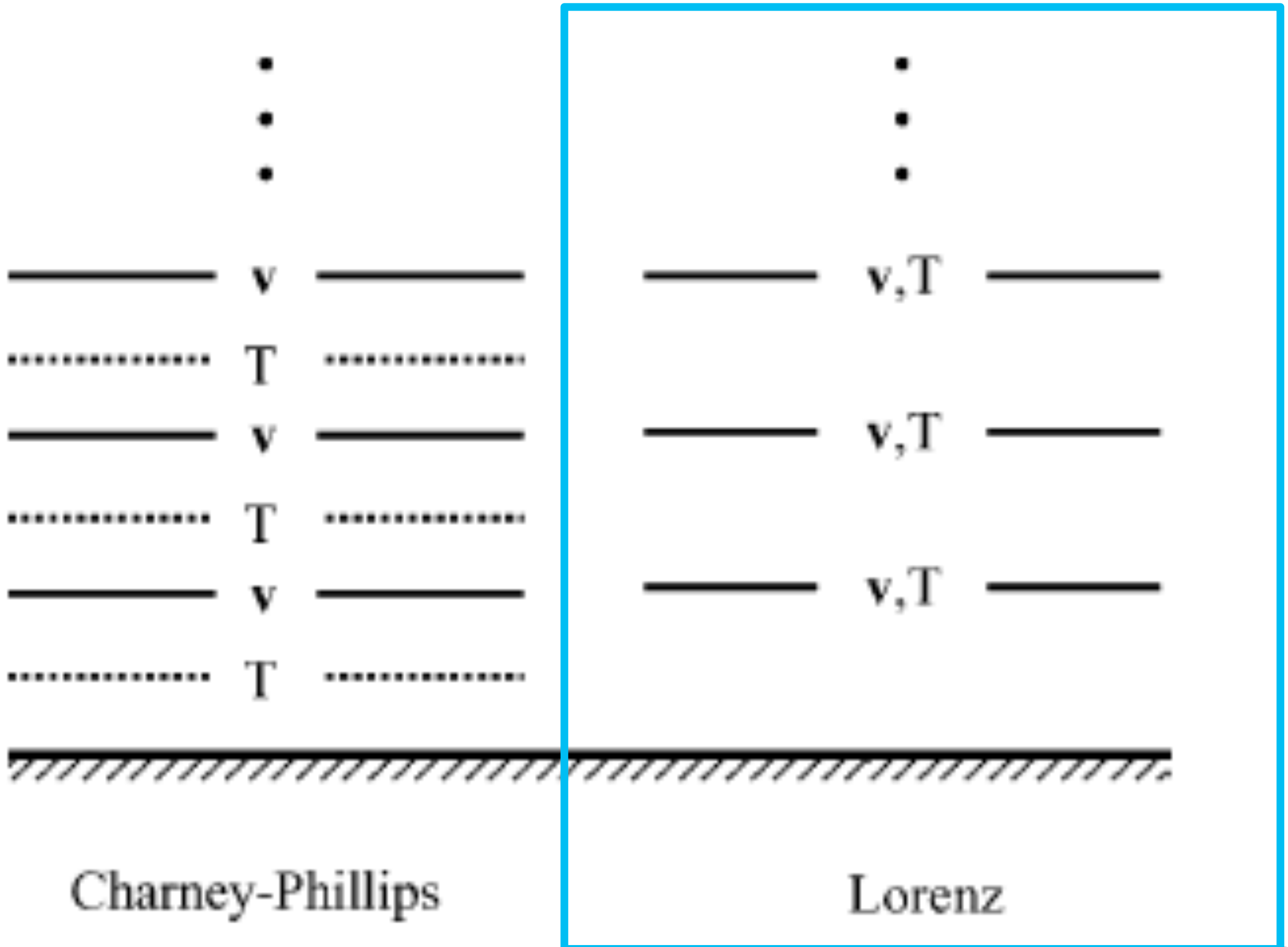

Space Discretization Principles

- Conservation of important properties of the continuous system aka “mimetic” approach in Comp. Math. (Arakawa 1966, 1972, …; Jacobson 2001; Janjic 1977, 1984, …; Sadourny, 1968, … ; Tripoli, 1992 …)

Space Discretization Principles

- Nonlinear energy cascade controlled through energy and enstrophy conservation
- A number of properties of differential operators preserved
- Quadratic conservative finite differencing
- A number of first order (including momentum) and quadratic quantities conserved
- Omega-alpha term, transformations between KE and PE
- Errors associated with representation of orography minimized
- Mass conserving positive definite monotone Eulerian tracer advection

Atmospheric Spectrum

- Numerical models generally generate excessive small scale noise
  - False nonlinear energy cascade (Phillips, 1954; Arakawa, 1966 … ; Sadourny 1975; …)
  - Other computational errors
- Historically, problem controlled by:
  - Removing spurious small scale energy by numerical filtering, dissipation
  - Preventing excessive noise *generation* by enstrophy and energy conservation (Arakawa, 1966 … , Janjic, 1977, 1984; Janjic et al., 2010) by design

Advection, divergence operators, each point talks to 8 neighbors

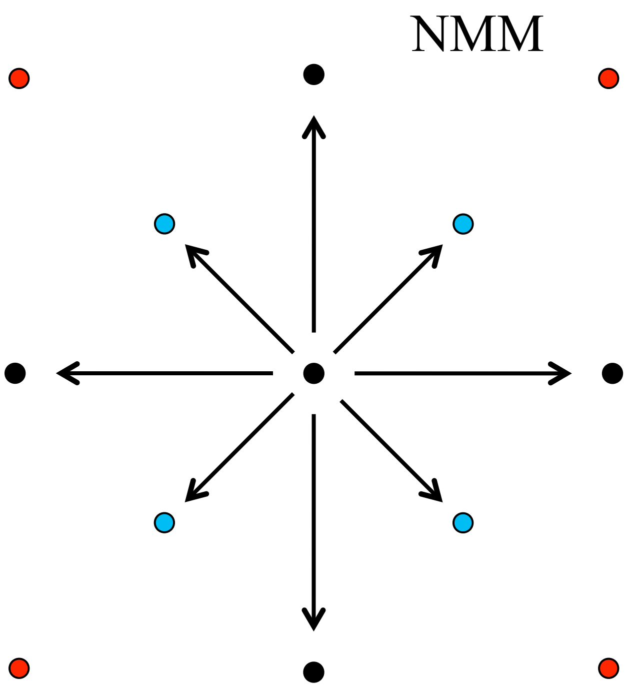

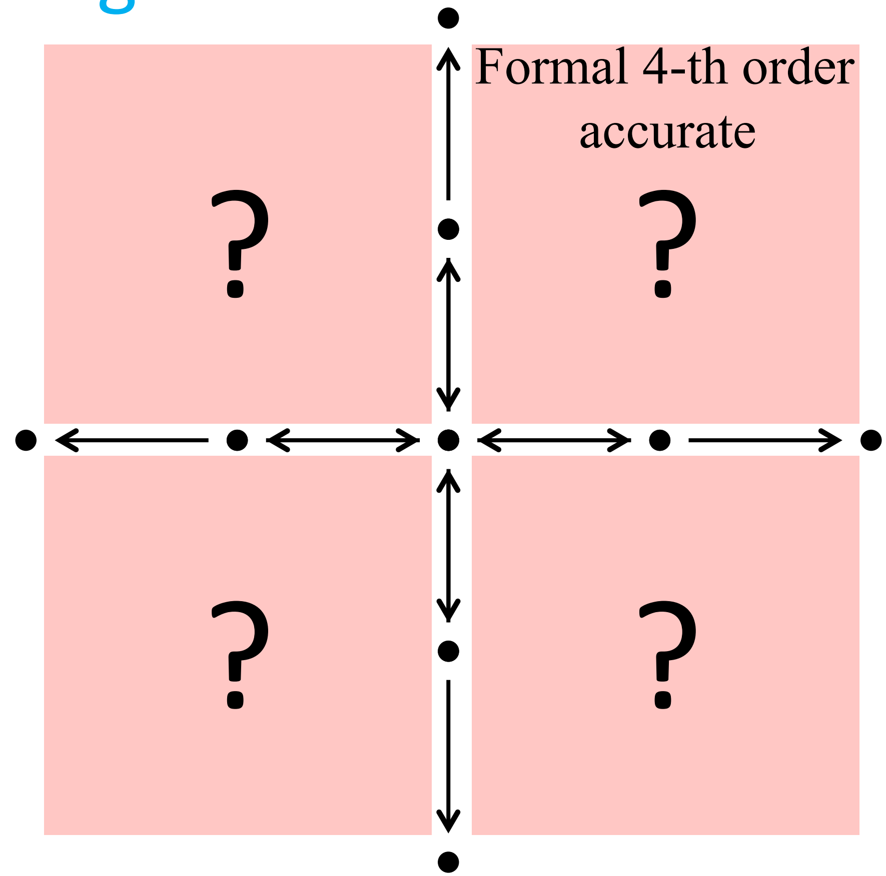

* E grid FD schemes also reformulated for, and used in ESMF compliant B grid model being developed

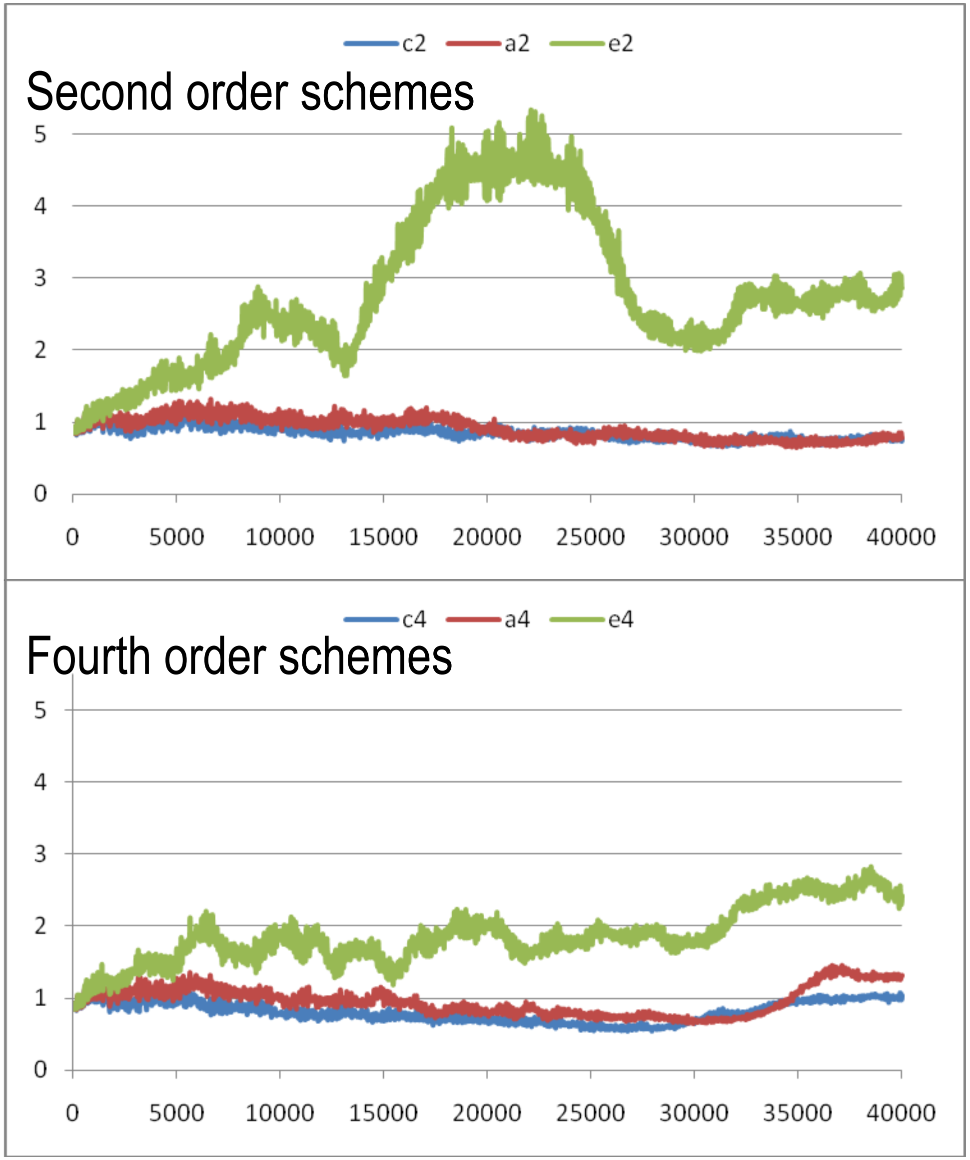

116 days

- Three sophisticated momentum advection schemes with identical linearized form, and therefore identical truncation errors and formal accuracy, but different nonlinear conservation properties. Janjic, 1984, MWR (blue); controlled energy cascade, but not enstrophy conserving, Arakawa, 1972, UCLA (red); energy and alternative enstrophy conserving, Janjic, 1984,MWR (green)
- Different nonlinear noise levels (green scheme) with identical formal accuracy and truncation error (Janjic et al., 2011, MWR)
- In nonlinear systems conservation more important than formal accuracy

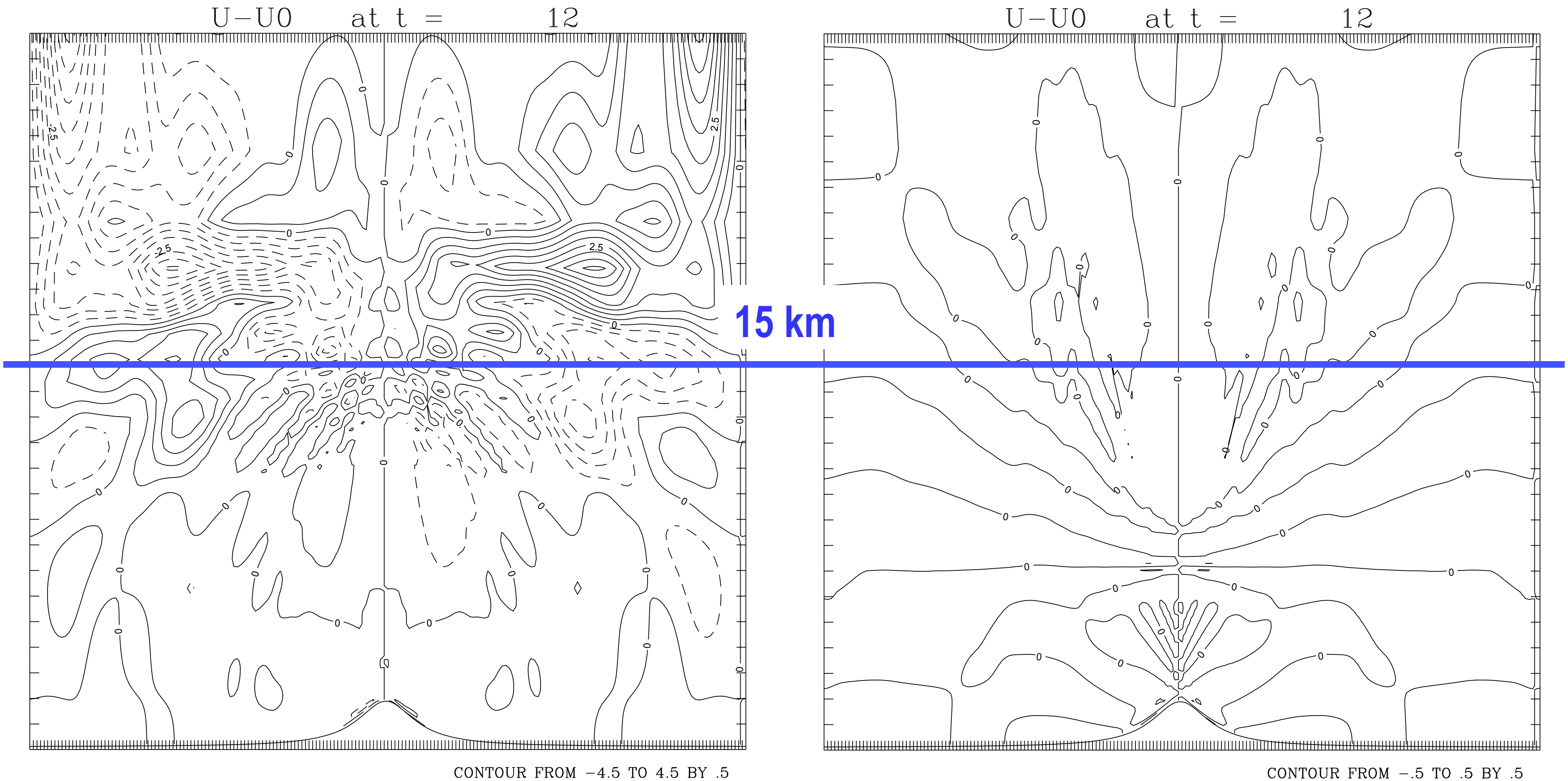

Wind component developing due to the spurious pressure gradient force in the sigma coordinate (left panel), and in the hybrid coordinate with the boundary between the pressure and sigma domains at about 400 hPa (right panel). Dashed lines represent negative values.

Example of nonphysical small scale energy source

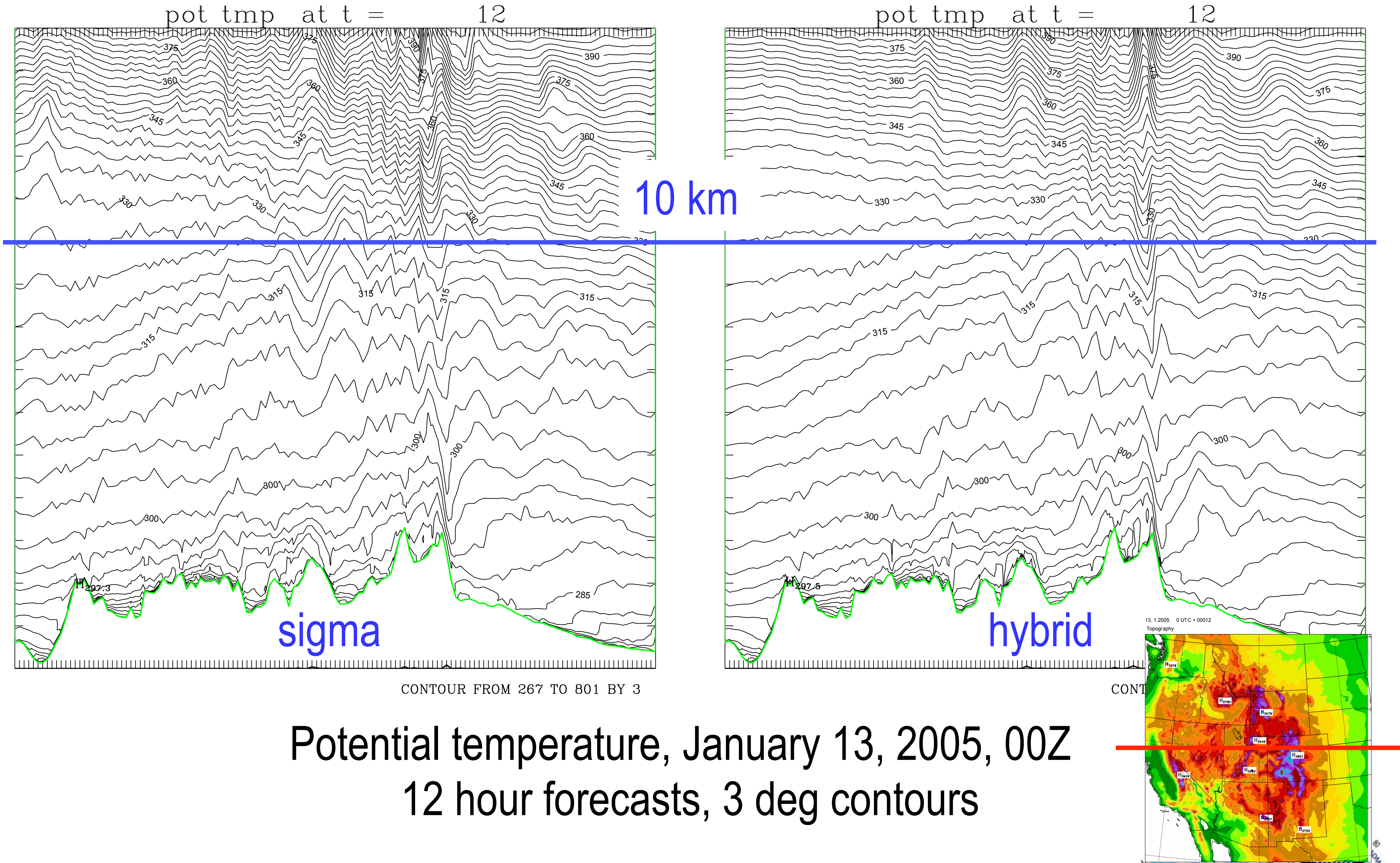

Potential temperature, January 13, 2005, 00Z
12 hour forecasts, 3 deg contours

Lateral Boundary Conditions

- Specified from the driving model along external boundaries
- 4-point averaging along first internal row (Mesinger and Janjic, 1974; Miyakoda and Rosati, 1977; Mesinger, 1977)
- Upstream advection area next to the boundaries from 2nd internal row
  - Advection well posed along the boundaries, no computational boundary condition needed
  - Dissipative
- HWRF internal nesting discussed elsewhere

Lateral Boundary Conditions

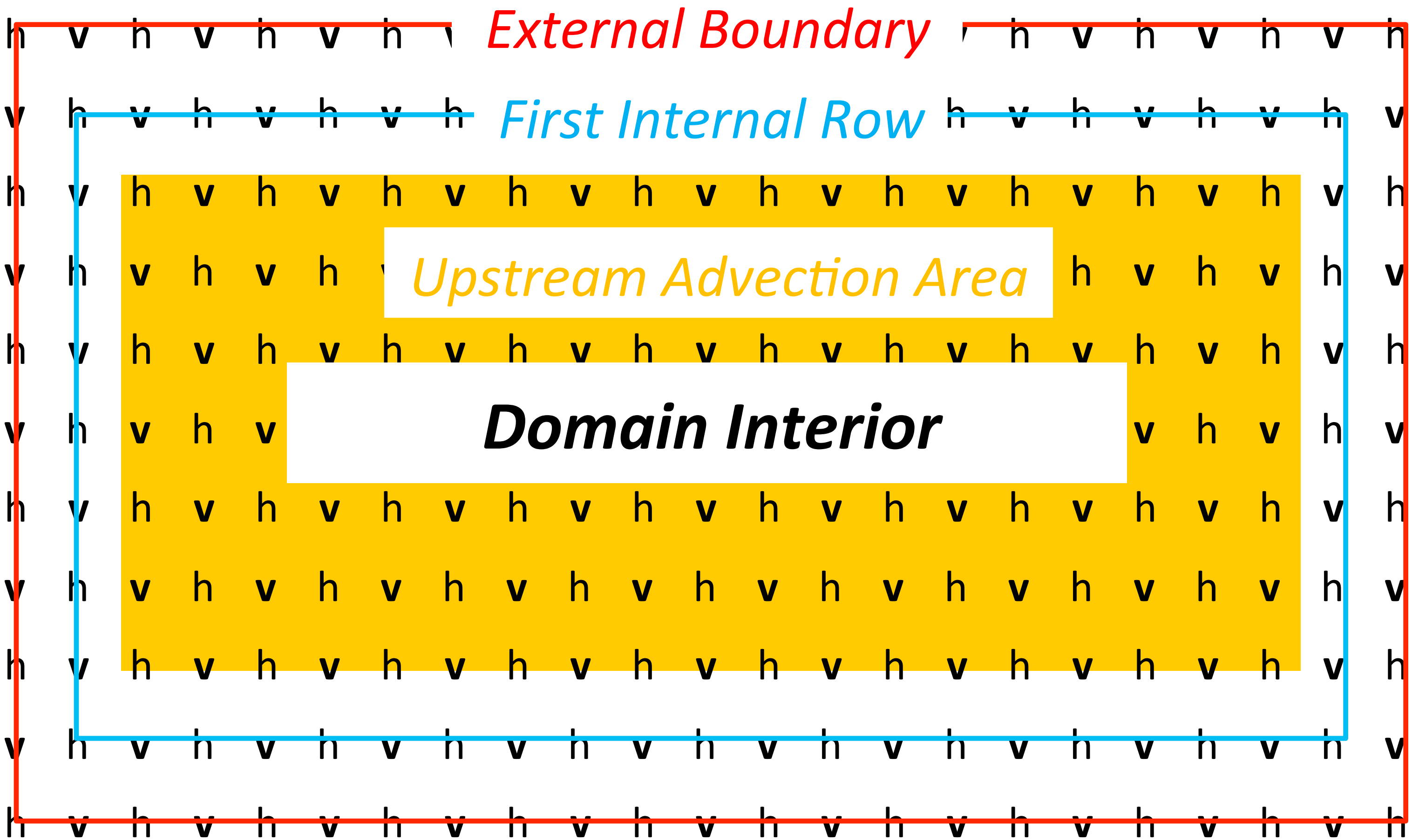

Time Integration

- Explicit where possible for accuracy, reduced communications on parallel computers
  - Horizontal advection of u, v, T, tracers (including q, cloud water, TKE …)
  - Coriolis force
- Implicit for fast processes that require a restrictively short time step for numerical stability, only in vertical columns, no impact on scalability
  - Vertical advection of u, v, T, tracers and vertically propagating sound waves
- No time splitting and no iterative time stepping schemes in basic dynamics equations for accuracy and computational efficiency

Horizontal advection and Coriolis Force

Non-iterative 2nd order Adams-Bashforth:

$$\frac{y^{\tau+1} - y^{\tau}}{\Delta t} = \frac{3}{2} f(y^{\tau}) - \frac{1}{2} f(y^{\tau-1})$$

Weak linear instability (amplification), can be tolerated in practice with short time steps, or stabilized by a slight off-centering as in the WRF-NMM.

$$\frac{y^{\tau+1} - y^{\tau}}{\Delta t} = 1.533 f(y^{\tau}) - 0.533 f(y^{\tau-1})$$

$$\frac{\partial u_j}{\partial t} = -C \frac{u_{j+1} - u_{j-1}}{2\Delta x}$$

$$C = 110\ ms^{-1},\ \Delta t = \frac{1}{3}\frac{\Delta x}{C}$$

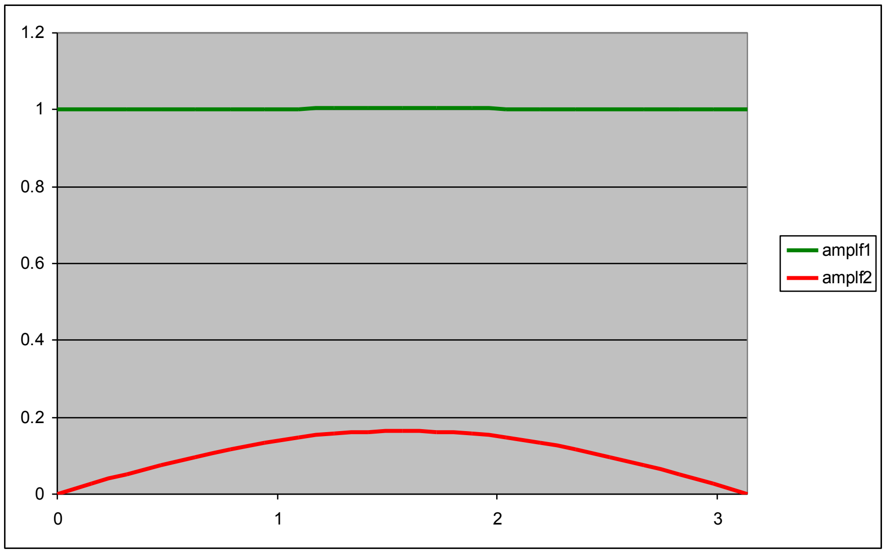

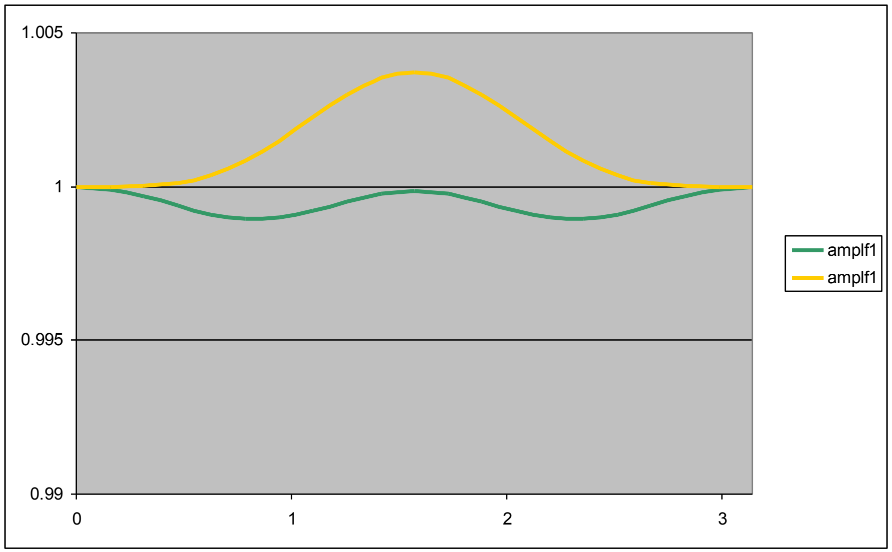

Amplification factors for the computational mode (red) and the meteorological mode in the Adams-Bashforth scheme. Wave number is shown along the abscissa.

Zoomed amplification factor near 1. The amplification factors of the modified Adams-Bashforth scheme (green), and the original one (orange)

Vertical Advection

Implicit Crank-Nicolson

$$\frac{y^{\tau+1} - y^{\tau}}{\Delta t} = \frac{1}{2}[f(y^{\tau+1}) + f(y^{\tau})]$$

Unconditionally computationally stable

Off-centering option, dissipative

$$\frac{y^{\tau+1} - y^{\tau}}{\Delta t} = \frac{1}{2}[af(y^{\tau+1}) + bf(y^{\tau})],\ a + b = 2$$

Advection of tracers

- New Eulerian advection replaced the old Lagrangian
  - Improved conservation of advected species, and more consistent with remainder of the dynamics
  - Reduces precipitation bias in warm season
- Advects sqrt(quantity) to ensure positivity
- Ensures monotonicity *a posteriori*

Advection of tracers

- Twice longer time steps than for the basic dynamics

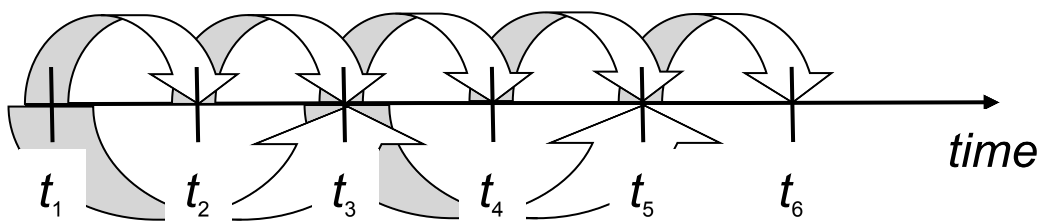

Advection only experiments of a prescribed pollutant tracer in a real atmospheric flow

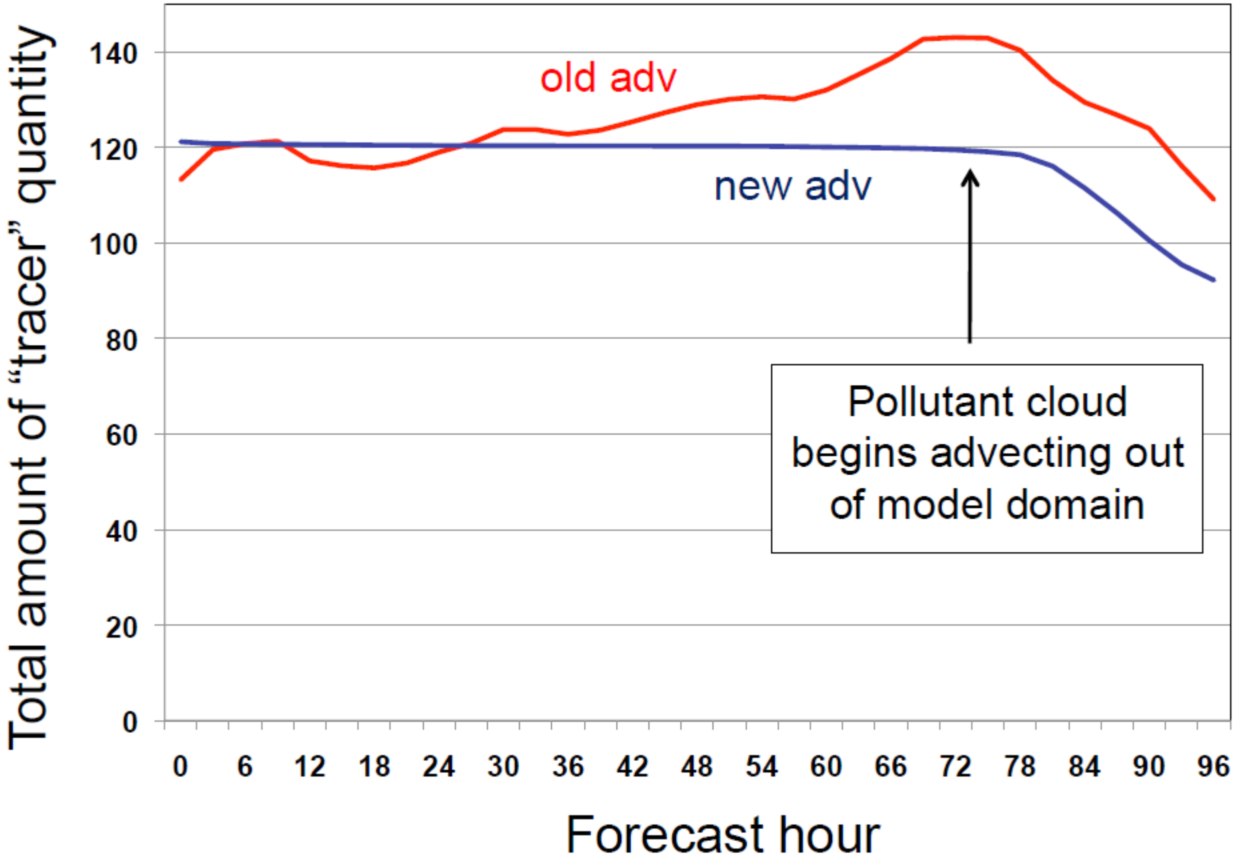

Courtesy Youhua Tang

Gravity Wave Terms

- Forward-Backward (Ames, 1968; Gadd, 1974; Janjic and Wiin-Nielsen, 1977; Janjic 1979)
  - Mass field computed from a forward time difference, while the velocity field comes from a backward time difference.
- 1D shallow water example

$$\frac{\partial u}{\partial t} = -g\frac{\partial h}{\partial x}, \frac{\partial h}{\partial t} = -H\frac{\partial u}{\partial x}$$

$$h^{\tau+1} = h^{\tau} - \Delta t\, H\frac{\partial u^{\tau}}{\partial x}$$

$$u^{\tau+1} = u^{\tau} - \Delta t\, g\frac{\partial h^{\tau+1}}{\partial x}$$

Mass field forcing to update wind from t +1 time

Vertically Propagating Sound Waves

- Actual computations hidden in a highly implicit algorithm
- In case of linearized equations in a vertical column (Janjic et al., 2001; Janjic, 2003, 2011), reduces to

$$\frac{p'^{\tau+1} - 2p'^{\tau} + p'^{\tau-1}}{\Delta t^2} = \frac{c_p}{c_v} R T_0 \frac{\partial^2 p'^{\tau+1}}{\partial z_0^2},$$

p' *deviation from basic state hydrostatic pressure*

Lateral Diffusion

- Following Smagorinsky (1963) (Janjic, 1990, MWR; Janjic et al. 2010)

$$K = (C_S\, l)^2 \Delta$$

C_S *Smagorinsky constant*, $\boxed{0.2 - 0.4}$

l *length scale*, $\propto$ *grid size*

Δ *deformation*

HWRF

$$\Delta = \left[2\left(\frac{\partial u}{\partial x} - \frac{\partial v \cos\varphi}{\partial y}\right)^2 + 2\left(\frac{\partial v}{\partial x} + \frac{\partial u \cos\varphi}{\partial y}\right)^2 + \boxed{4\left(\frac{\partial w}{\partial x}\right)^2 + 4\left(\frac{\partial w}{\partial y}\right)^2 + \cancel{2C'TKE}}\right]^{1/2}$$

2D Divergence Damping

- Dispersion of gravity-inertia waves alone can explain linear geostrophic adjustment on an infinite plain
- "In a finite domain, unless viscosity is introduced, gravity waves will forever 'slosh' without dissipating." (e.g., Vallis, 1992, JAS)
- Numerical experiments by Farge and Sadourny (1989, J.Fluid.Mech.) strongly support the idea of dissipative geostrophic adjustment

2D Divergence Damping

$$D_l = \frac{1}{3}\frac{\delta_x(\overline{\Delta\pi}^x\, u\,\Delta y) + \delta_y(\overline{\Delta\pi}^y\, v\,\Delta x)}{\Delta A} + \frac{2}{3}\frac{\delta_{x'}(\Delta\pi\, u' d_n') + \delta_{y'}(\Delta\pi\, v' d_n')}{\Delta A'}$$

$$\Delta\pi\, u' d_n' = \overline{\overline{\Delta\pi}^x\, u\,\Delta y + \overline{\Delta\pi}^y\, v\,\Delta x}^{y'}$$

$$\Delta\pi\, v' d_n' = \overline{-\overline{\Delta\pi}^x\, u\,\Delta y + \overline{\Delta\pi}^y\, v\,\Delta x}^{x'}$$

π – *hydrostatic pressure*

$$\Delta A = 4\Delta x\Delta y$$

$$\Delta A' = 2\Delta x\Delta y$$

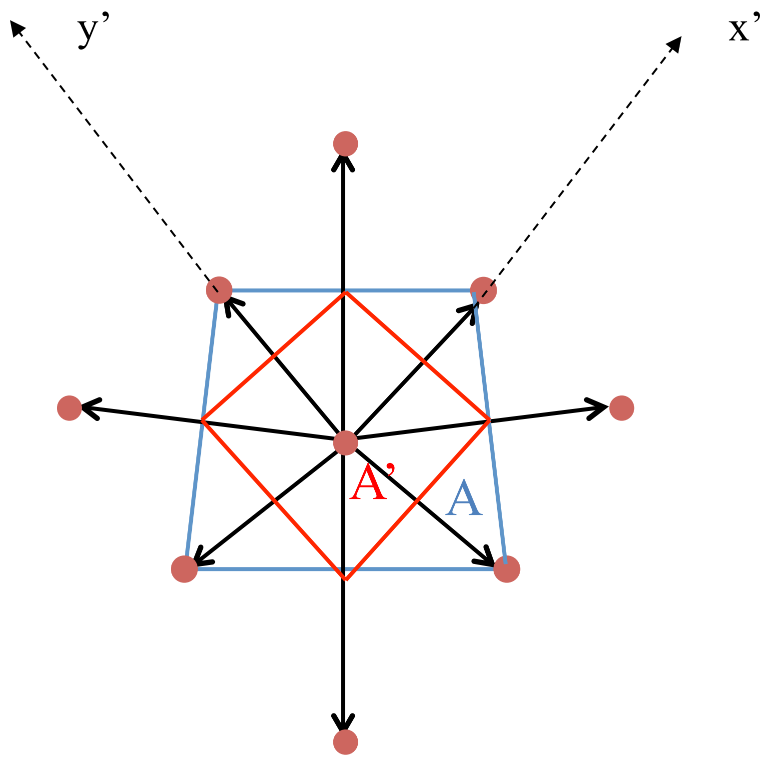

2D Divergence damping

- Divergence damping damps both internal and external modes

$$\Delta\pi \frac{\partial u}{\partial t} = K_1\, \delta_x D_l$$

$$\Delta\pi \frac{\partial v}{\partial t} = K_1\, \delta_y D_l$$

2D Divergence Damping

- External mode divergence

$$D_{ext} = \sum_{bottom}^{top} D_l$$

- External mode divergence damping

$$\Delta\pi \frac{\partial u}{\partial t} = K_2 \frac{\Delta\pi}{\mu} \delta_x D_{ext}$$

$$\Delta\pi \frac{\partial v}{\partial t} = K_2 \frac{\Delta\pi}{\mu} \delta_y D_{ext}$$

2D Divergence Damping

- External mode damping combined with divergence damping, enhanced damping of the external mode

$$\frac{\partial u}{\partial t} = \frac{K_1}{\Delta\pi}\delta_x D_l + \frac{K_2}{\mu}\delta_x D_{ext}$$

$$\frac{\partial v}{\partial t} = \frac{K_1}{\Delta\pi}\delta_y D_l + \frac{K_2}{\mu}\delta_y D_{ext}$$

Dynamics formulation tested on various scales

Warm bubble

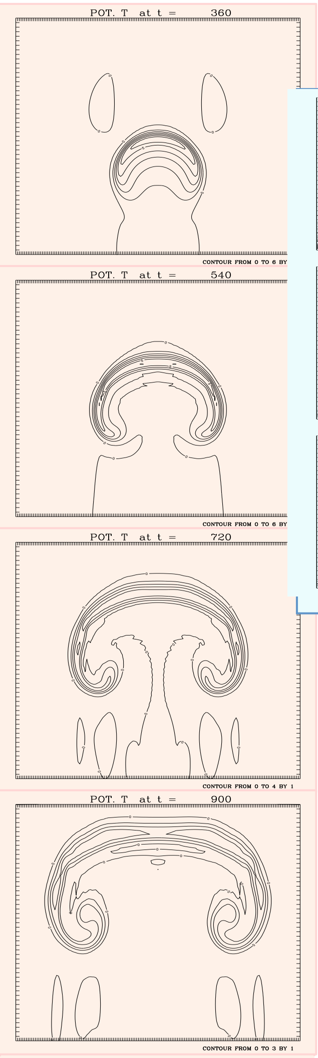

Cold bubble

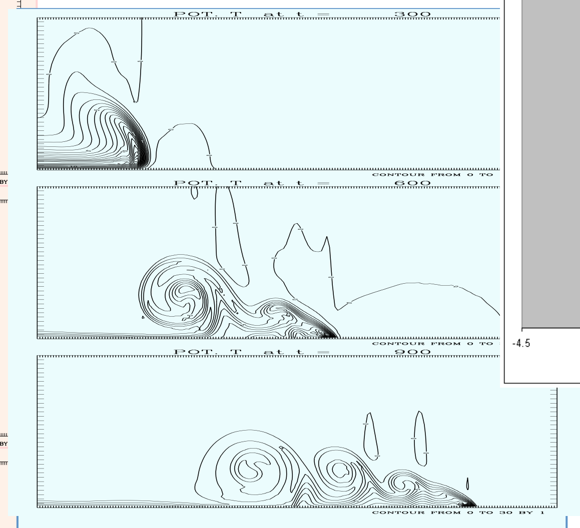

Decaying 3D turbulence

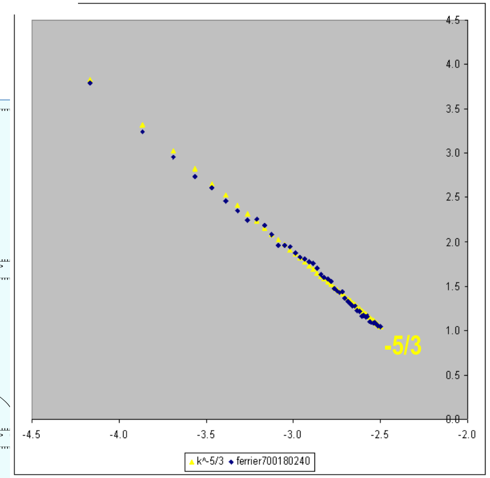

Mountain waves

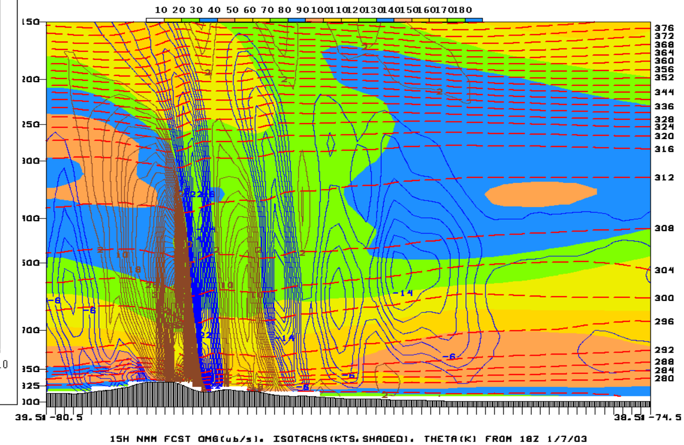

Atmospheric spectra

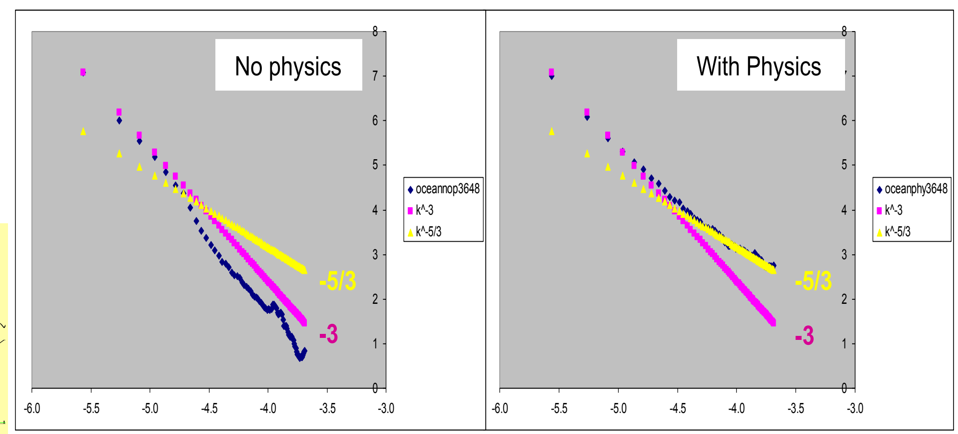

Convection

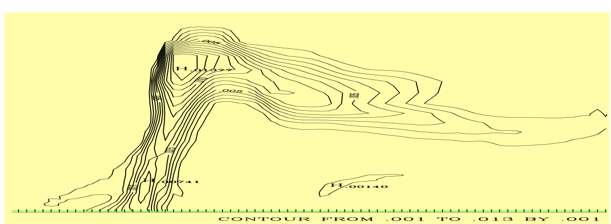

4km resolution, no parameterized convection

2004

Breakthrough that lead to application of “convection allowing” resolution for storm prediction

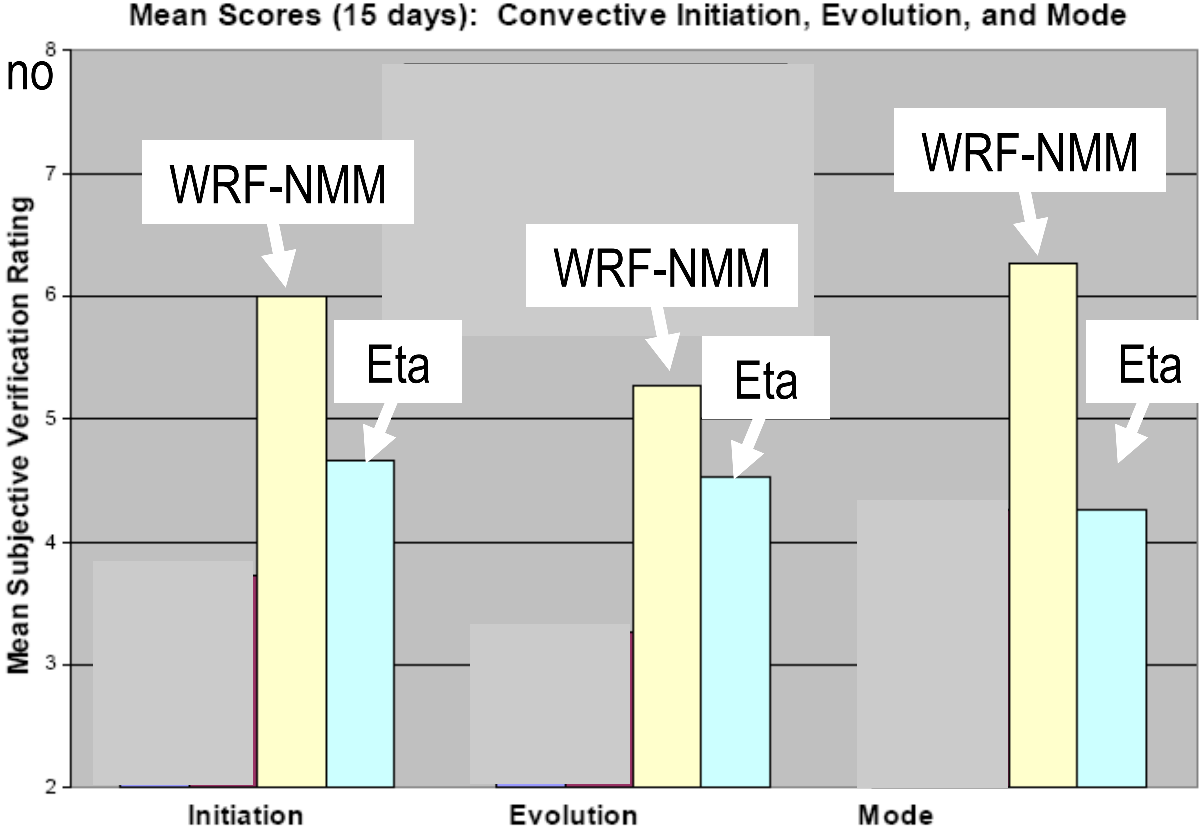

Fig. 5. Mean subjective verification ratings for the operational Eta model and the 3 high-resolution configurations of the WRF model, for categories of convective initiation, evolution, and mode, for the 15 days when all 4 models were available

17.1 EXAMINATION OF SEVERAL DIFFERENT VERSIONS OF THE WRF MODEL FOR THE PREDICTION OF SEVERE CONVECTIVE WEATHER: THE SPC/NSSL SPRING PROGRAM 2004

Steven J. Weiss[*,1], J. S. Kain[2], J. J. Levit[1], M. E. Baldwin[2], and D. R. Bright[1]

[1]NOAA/NWS/Storm Prediction Center
[2]University of Oklahoma/CIMMS/National Severe Storms Laboratory

22nd Conference on Severe Local Storms, October 3-8, 2004, Hyannis, MA.

Summary

- Robust, reliable, fast
- Extension of NWP methods developed and refined over a decades-long period into the nonhydrostatic realm
- Utilized at NCEP in the HWRF, Hires Window and Short Range Ensemble Forecast (SREF)operational systems

Horizontal Coordinate System, Rotated Lat-Lon

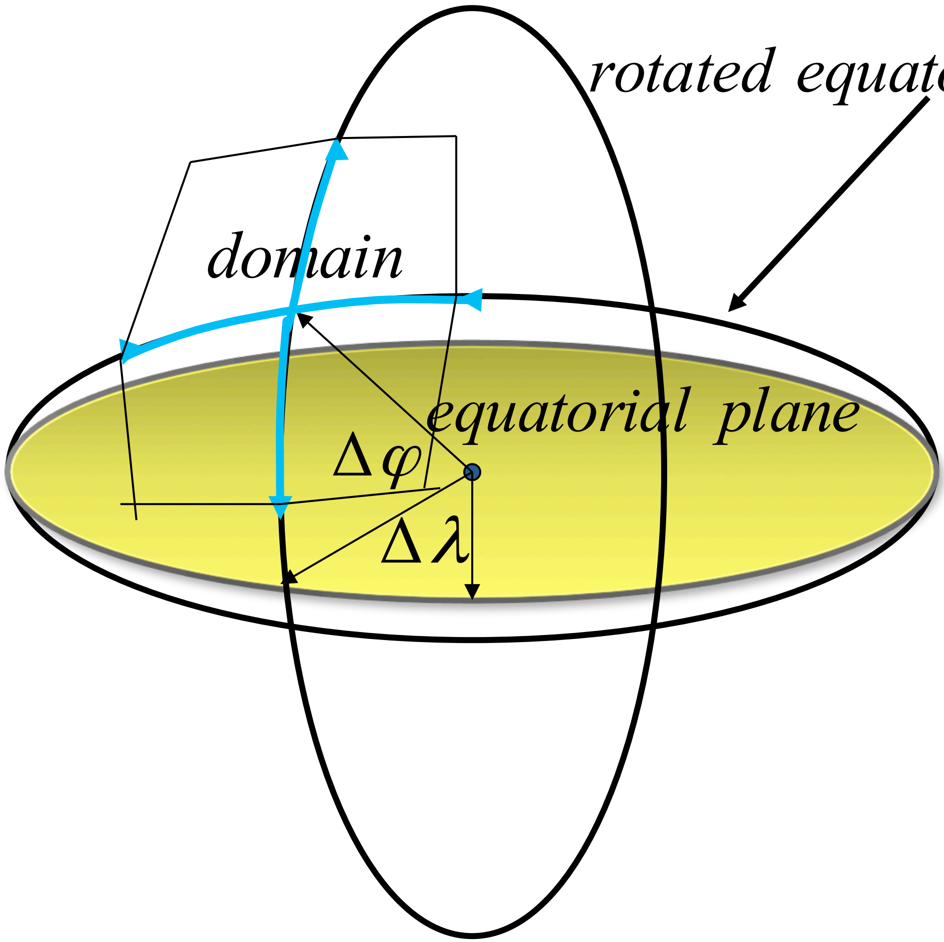

$$10^0 N < \varphi < 70^0 N$$

$$\Delta x \propto \cos(\varphi)$$

$$lat - lon$$

$$\cos(70^0)/\cos(10^0) = 0.3473$$

$$rotated\ lat - lon$$

$$\cos(30^0)/\cos(0^0) = 0.866$$